mathematics

MDPI

Article

Mathematical Study for Chikungunya Virus with Nonlinear General Incidence Rate

Salah Alsahafi * and Stephen Woodcock

School of Mathematical and Physical Sciences, University of Technology, 15 Broadway, Ultimo, Sydney, NSW 2007, Australia; Stephen.Woodcock@uts.edu.au
* Correspondence: SALAH.ALSAHAFI@student.uts.edu.au

Abstract: In this article, we examine the dynamics of a Chikungunya virus (CHIKV) infection model with two routes of infection. The model uses four categories, namely, uninfected cells, infected cells, the CHIKV virus, and antibodies. The equilibrium points of the model, which consist of the free point for the CHIKV and CHIKV endemic point, are first analytically determined. Next, the local stability of the equilibrium points is studied, based on the basic reproduction number ($\mathcal{R}_0$) obtained by the next-generation matrix. From the analysis, it is found that the disease-free point is locally asymptotically stable if $\mathcal{R}_0 \leq 1$, and the CHIKV endemic point is locally asymptotically stable if $\mathcal{R}_0 > 1$. Using the Lyapunov method, the global stability analysis of the steady-states confirms the local stability results. We then describe our design of an optimal recruitment strategy to minimize the number of infected cells, as well as a nonlinear optimal control problem. Some numerical simulations are provided to visualize the analytical results obtained.

Keywords: Chikungunya virus; cellular infection; general incidence rate; LaSalle's invariance principle; Lyapunov stability; optimal control

Citation: Alsahafi, S.; Woodcock, S. Mathematical Study for Chikungunya Virus with Nonlinear General Incidence Rate. *Mathematics* **2021**, *9*, 2186. https://doi.org/10.3390/math9182186

Academic Editor: Mikhail Kolev

Received: 4 July 2021
Accepted: 3 September 2021
Published: 7 September 2021

1. Introduction

The Chikungunya virus (CHIKV) belongs to the Togaviridae family of the genus Alphavirus [1,2]. It takes the form of an enveloped spherical viral particle with a diameter of 65 nm, containing a single RNA of positive polarity, encoding two polyproteins. The RNA is directly infectious and, therefore, serves as both a genome and messenger RNA. The 11,000 to 12,000 bases of its genome ultimately allow the synthesis of nine proteins, obtained after cleavage of the polyproteins by viral and cellular proteases. At the end of the viral cycle, which includes protein synthesis, replication, and assembly of viral particles, the viral proteins bud on the plasma membrane of the infected cell, and then penetrate the membrane. The virus is transmitted to humans when anticoagulant saliva is injected into the blood of the person bitten by an infected mosquito [1,2]. We now know that the virus does not infect circulating blood cells, but rather, macrophages and adherent cells (endothelial, epithelial, fibroblast).

In [3], Sourisseau et al. first adapted tools (flow cytometry, immunofluorescence, electron microscopy, etc.) to specify and quantify the CHIKV. Therefore, they proved in vitro that CHIKV does not replicate in circulating blood cells (lymphocytes, monocytes), but that it replicates in macrophages (phagocytic cells which are of blood origin but localized in tissues). These cells itself infect tissues, such as muscles and joints. The CHIKV also infects the so-called "adherent" cells, such as endothelial cells, epithelial cells, and fibroblasts. A study conducted by Ozden at al. [4] has shown that, in infected people, certain cells present in muscle tissue are targets of the CHIKV. Their work was based on the study of patient biopsies. They found that, in a biopsy taken at an acute stage of the disease from one patient, and in another taken at a later stage from another patient, the precursor cells of muscle cells—the satellite cells—were infected with the virus. In addition, these cells have been found, in cell culture, to be very permissive to the virus. The authors are now

trying to discover if these cells play the role of a "reservoir" of the virus, which would explain the recurrence of muscle pain observed in some patients. [5] stated that like any virus, the CHIKV enters its host's cells and uses the cellular machinery there to replicate. In particular, it is shown that this arbovirus replicates in macrophages, cells of the immune system specializing in phagocytosis and present in several tissues and organs. On the other hand, it does not reproduce in the T and B lymphocytes which are circulating in the blood. CHIKV also infects epithelial cells (organ wall), endothelial cells (inner wall of blood vessels), as well as cells of fibrous tissues (fibroblasts).

The contribution of mathematics is made initially through modelling [6–14]. This stage of mathematical modelling makes it possible to test, without wasting time or expense, the control measures that are envisaged: preventive measures, isolation of patients, treatments, vaccinations, and so forth. The model, nevertheless, does not completely reflect reality and is not intended to reproduce it in full. It must reproduce the characteristics of the phenomenon studied according to the objectives set for the framework of the study as well as possible. Modelling such a phenomenon consists of applying mathematical tools to a fragment of reality. It is transforming a need into equations, trying as much as possible to account for the constraints identified. Modelling is the most delicate, the longest, and often the most perilous step. Indeed, it is necessary to successfully understand the real problem to try to propose a suitable model. The first proposed attempt only very rarely meets expectations, and several modifications then follow, until a model is reached that groups together and reflects the maximum number of constraints that the real phenomenon must observe. If this step is neglected or omitted, if the constraints are not well-posed, then one ends up with a mathematical formulation which does not correspond to the problem. The resolution of the mathematical problem then provides a solution not suited to the concrete problem. However, if the problem is well-posed, then the next step is to solve the problem, that is, to analyse the model to understand, predict, and act.

Researchers have proposed several mathematical systems describing the CHIKV dynamics (see, e.g., [15–21]). Most of the proposed models were designed to describe the disease transmission from mosquitoes to human populations. In [22], Wang and Liu proposed a mathematical model which assumed that the contamination of a monocyte (a type of leukocyte, or white blood cell) occurs when a monocyte comes into contact with the virus. Several mathematical models have been proposed using both cellular and viral infections [13,20,23–25]. Elaiw et al. in [17] proposed and studied a mathematical model with two routes of infection. Later, Elaiw et al. [18,19] studied both routes of infection in a CHIKV dynamics model with Holling type-II incidence rates. Several forms of incidence rates have been applied in epidemic models [26].

In the present paper, we reconsider the mathematical system given in [18] by Elaiw et al. by considering two main changes relevant to an applied perspective:

1. Considering the adherent cells as the main target for CHIKV and not monocytes, as mentioned in a series of previous papers [15–20].
2. Considering general nonlinear increasing incidence rates with respect to the uninfected cells. This choice is motivated by the fact that the number of effective contacts between infective cells and susceptible cells or between the virus and susceptible cells may increase at high infective levels due to crowding of susceptible cells.

The basic reproduction number, $\mathcal{R}_0$, was determined based on the next-generation matrix method [27–29]. Local stability analysis was carried out using local linearisation. Global stability analysis of the steady-states was studied using Lyapunov stability. We proved that the CHIKV-free equilibrium point, E_0, is globally asymptotically stable if $\mathcal{R}_0 \leq 1$ and the infected equilibrium point, E_1, is globally asymptotically stable if $\mathcal{R}_0 > 1$. Furthermore, we proposed an optimal recruitment strategy to optimize the number of infected cells. We designed an optimal control problem. The resolution of the state system was reached by applying an improvement to the Gauss-Seidel-like implicit finite-difference method. The adjoint system was solved using a first-order backward-difference. Some numerical simulations confirming the obtained results are given.

2. Mathematical Model and Results

Consider the following mathematical model describing the CHIKV dynamics with two routes of infection which is a generalization of the mathematical model given in [18].

$$\begin{cases} \dot{s} &= \Gamma - \delta s - \eta_1 p f(s) - \eta_2 y f(s), \\ \dot{y} &= \eta_1 p f(s) + \eta_2 y f(s) - \epsilon y, \\ \dot{p} &= \pi y - cp - rxp, \\ \dot{x} &= \lambda + \rho xp - mx. \end{cases} \tag{1}$$

The variables s, y, p and x describe the number of uninfected and infected cells, the CHIKV virus, and antibodies, respectively. The model parameters are nonnegative and are described as follows.

Parameter	Description
Γ	uninfected cells recruitment rate
δ	Uninfected cells mortality rate
ϵ	Infected cells mortality rate
c	CHIKV mortality rate
m	Antibodies loss rate
π	Generation rate of the virus by infected cells
r	Rate at which Antibodies attack the virus
λ	Antibodies expansion rate
ρ	Proliferate rate of antibodies, once antigen is encountered
η_1, η_2	Incidence rate constants

Note that $(\eta_1 p f(s) + \eta_2 y f(s))$ represents the number of cells disappearing from recruitment in the susceptible compartment and entering into an infected compartment, where f is a nonlinear increasing function.

Using nonlinear incidence rates of the form $\eta_1 f(s)p$ and $\eta_2 f(s)y$ into this model is important because the number of effective contacts between infective cells and susceptible cells may increase at high infective levels due to crowding of susceptible cells. If the function $f(s)$ is increasing for large values of s, used for interpreting the "psychological" effects: for high number of susceptible cells, the infection risk increase as the number of susceptible cells increases, since the total number of cells may tend to increase the number of contacts.

Let $s_0 = \dfrac{\Gamma}{\delta}$ and $x_0 = \dfrac{\lambda}{m}$. We make the following assumption that will be used in the rest of the paper.

Assumption 1. *f is an increasing, nonnegative $C^1(\mathbb{R}_+)$ function such that $f(0) = 0$ and $f(s_0) < \dfrac{\epsilon}{\eta_2}$.*

Assumption 1 states that the CHIKV-cell and the infected-cell incidence rates increase with the number of susceptible cells. Assumption 1 also considers that no CHIKV-cell and infected-cell infections can take place in the absence of susceptible cells.

The classical Monod functions can be used to express the transmission rate of infections from infected to susceptible cells as well as from CHIKV to susceptible cells:

$$f(s) = \frac{\bar{\mu} s}{k + s},$$

where $\bar{\mu}$ represents the transmission rates of the disease and k is the Monod constant which is proportional both to the number of CHIKV pathogens and infected cells when the saturated incidence rate is $\bar{\mu}/2$.

The last condition of Assumption 1 is of a mathematical artifice that we used to prove the existence and uniqueness of the infected equilibrium point.

2.1. Basic Properties

First note that $\dot{s} \leq \Gamma - \delta s$; then, one can easily deduce that

Lemma 1. *if* $s(0) \leq s_0$, *we have* $s(t) \leq s_0 + \big(s(0) - s_0\big)e^{-\delta t} \leq s_0, \quad \forall t \geq 0.$

The system (1) admits non-negative bounded solutions. In particular,

Lemma 2. *there exist* $M_1, M_2, M_3 > 0$ *such that*

$$\Omega = \{(s, y, p, x) \in \mathbb{R}^4_{\geq 0} : 0 \leq s, y \leq M_1, 0 \leq p \leq M_2, 0 \leq x \leq M_3\}$$

is a positively invariant bounded set for system (1)

.

Proof. Note that

$$\begin{aligned}
\dot{s} \mid_{s=0} &= \Gamma > 0,\\
\dot{y} \mid_{y=0} &= \eta_1 p f(s) \geq 0, \ \forall\, s, p \geq 0,\\
\dot{p} \mid_{p=0} &= \pi y \geq 0, \ \forall\, y \geq 0,\\
\dot{x} \mid_{x=0} &= \lambda > 0.
\end{aligned}$$

Consider $S_1(t) = s(t) + y(t)$ and $S_2(t) = p(t) + \dfrac{r}{\rho}x(t)$. Then, one has

$$\dot{S}_1(t) = \Gamma - \delta s(t) - \epsilon y(t) \leq \Gamma - \gamma_1(s(t) + y(t)) = \Gamma - \gamma_1 S_1(t),$$

where $\gamma_1 = \min\{\delta, \epsilon\}$. Hence $S_1(t) \leq M_1$, if $S_1(0) \leq M_1$, with $M_1 = \dfrac{\Gamma}{\gamma_1}$. Therefore, $0 \leq s(t), y(t) \leq M_1$ if $0 \leq s(0) + y(0) \leq M_1$. Furthermore, one has

$$\begin{aligned}
\dot{S}_2(t) &= \pi y(t) - c p(t) + \frac{r}{\rho}\lambda - \frac{mr}{\rho}x(t)\\
&\leq \pi M_1 + \frac{r}{\rho}\lambda - \gamma_2\left(p(t) + \frac{r}{\rho}x(t)\right)\\
&= \pi M_1 + \frac{r}{\rho}\lambda - \gamma_2 S_2(t),
\end{aligned}$$

where, $\gamma_2 = \min\{c, m\}$. Then $S_2(t) \leq M_2$, if $S_2(0) \leq M_2$, with $M_2 = \dfrac{\pi M_1 + \dfrac{r}{\rho}\lambda}{\gamma_2}$. As all variables are nonnegative, therefore, $0 \leq p(t) \leq M_2$ and $0 \leq x(t) \leq M_3$ if $0 \leq p(0) + \dfrac{r}{\rho}x(0) \leq M_2$, with $M_3 = \dfrac{\rho M_2}{r}$. □

2.2. Basic Reproduction Number and Equilibrium Points

The basic reproduction rate is a dimensionless quantity which allows the measurement of the ability of an infectious cell to spread infection through a given cell's population immediately after its introduction. From a mathematical point of view, it allows, under certain conditions, the stability of the points of equilibrium of a dynamic system to be established.

Diekmann et al. [27,28] designed a way to calculate the basic reproduction number $\mathcal{R}_0$, named the next-generation matrix method, and this was adapted by Van den Driessche and Watmough [29].

Here, $F = \begin{pmatrix} \eta_2 f(s_0) & \eta_1 f(s_0) & 0 \\ 0 & 0 & 0 \\ 0 & 0 & 0 \end{pmatrix}$ and $V = \begin{pmatrix} \epsilon & 0 & 0 \\ -\pi & rx_0 + c & 0 \\ 0 & -\rho x_0 & m \end{pmatrix}$. The determinant of V is given by $\det(V) = m\epsilon(rx_0 + c) > 0$; thus,

$$V^{-1} = \frac{1}{m\epsilon(rx_0 + c)} \begin{pmatrix} m(rx_0 + c) & 0 & 0 \\ m\pi & m\epsilon & 0 \\ \pi\rho x_0 & \epsilon\rho x_0 & \epsilon(rx_0 + c) \end{pmatrix}$$ and the next-generation matrix is given by

$$FV^{-1} = \frac{1}{m\epsilon(rx_0 + c)} \begin{pmatrix} m(rx_0 + c)\eta_2 f(s_0) + m\pi\eta_1 f(s_0) & m\epsilon\eta_1 f(s_0) & 0 \\ 0 & 0 & 0 \\ 0 & 0 & 0 \end{pmatrix}.$$

Then, the basic reproduction number of system (1) is calculated as the spectral radius of the matrix FV^{-1}:

$$\mathcal{R}_0 = \frac{m(rx_0 + c)\eta_2 f(s_0) + m\pi\eta_1 f(s_0)}{m\epsilon(rx_0 + c)} = \frac{\eta_2 f(s_0)}{\epsilon} + \frac{\pi\eta_1 f(s_0)}{\epsilon(rx_0 + c)}.$$

Lemma 3. • *If $\mathcal{R}_0 \leq 1$, then (1) admits only $E_0 \in \Omega$ as an equilibrium point.*

• *If $\mathcal{R}_0 > 1$, then (1) admits two equilibrium points, $E_0 \in \Omega$ and $E_1 \in \overset{\circ}{\Omega}$, and here, $\overset{\circ}{\Omega}$ represents the interior of the set Ω.*

Proof. Let $E(s, y, p, x)$ be an equilibrium point satisfying

$$0 = \Gamma - \delta s - \eta_1 p f(s) - \eta_2 y f(s), \tag{2}$$
$$0 = \eta_1 p f(s) + \eta_2 y f(s) - \epsilon y, \tag{3}$$
$$0 = \pi y - cp - rxp, \tag{4}$$
$$0 = \lambda + \rho x p - mx. \tag{5}$$

The resolution of Equations (2)–(5) gives us the CHIKV-free equilibrium point $E_0 = (s_0, 0, 0, x_0)$.

Moreover, we have

$$\begin{aligned} x &= \frac{\lambda}{m - \rho p}, \\ y &= \frac{cp + rxp}{\pi} = \frac{cp}{\pi} + \frac{r\lambda p}{\pi(m - \rho p)}, \\ s &= \frac{\Gamma - \epsilon y}{\delta} = s_0 - \frac{c\epsilon p}{\pi\delta} - \frac{r\lambda\epsilon p}{\pi\delta(m - \rho p)}, \\ \eta_1 p f(s) &= (\epsilon - \eta_2 f(s))y. \end{aligned}$$

We define the function

$$\begin{aligned} g(p) &= \eta_1 f(s) + (\eta_2 f(s) - \epsilon)\frac{y}{p} \\ &= \eta_1 f\Big(s_0 - \frac{c\epsilon p}{\pi\delta} - \frac{r\lambda\epsilon p}{\pi\delta(m - \rho p)}\Big) \\ &\quad + \Big(\eta_2 f\Big(s_0 - \frac{c\epsilon p}{\pi\delta} - \frac{r\lambda\epsilon p}{\pi\delta(m - \rho p)}\Big) - \epsilon\Big)\Big(\frac{c}{\pi} + \frac{r\lambda}{\pi(m - \rho p)}\Big). \end{aligned}$$

Then, we obtain

$$\begin{aligned} g(0) &= \eta_1 f(s_0) + (\eta_2 f(s_0) - \epsilon)\frac{cm + r\lambda}{\pi m} \\ &= \epsilon\frac{cm + r\lambda}{\pi m}\Big(\frac{\eta_2 f(s_0)}{\epsilon} + \frac{\pi m\eta_1 f(s_0)}{\epsilon(cm + r\lambda)} - 1\Big) \\ &= \epsilon\frac{cm + r\lambda}{\pi m}(\mathcal{R}_0 - 1) > 0 \quad \text{if} \quad \mathcal{R}_0 > 1. \end{aligned}$$

Now, we have $\lim_{p\to(m/\rho)^-}\Big(s_0-\frac{c\epsilon p}{\pi\delta}-\frac{r\lambda\epsilon p}{\pi\delta(m-\rho p)}\Big)=-\infty$, and then, $\lim_{p\to(m/\rho)^-}\eta_1 f\Big(s_0-\frac{c\epsilon p}{\pi\delta}-\frac{r\lambda\epsilon p}{\pi\delta(m-\rho p)}\Big)<0$ and $\lim_{p\to(m/\rho)^-}\eta_2 f\Big(s_0-\frac{c\epsilon p}{\pi\delta}-\frac{r\lambda\epsilon p}{\pi\delta(m-\rho p)}\Big)<0$. One deduces, therefore, that

$$\lim_{p\to(m/\rho)^-} g(p)<0.$$

The derivative of the function g is given by

$$\begin{aligned} g'(p) &= -\eta_1\Big(\frac{c\epsilon}{\delta\pi}+\frac{\epsilon r\lambda}{\delta\pi}\frac{m}{(m-\rho p)^2}\Big)f'\Big(s_0-\frac{c\epsilon p}{\pi\delta}-\frac{r\lambda\epsilon p}{\pi\delta(m-\rho p)}\Big)\\ &-\eta_2\Big(\frac{c}{\pi}+\frac{r\lambda}{\pi(m-\rho p)}\Big)\Big(\frac{c\epsilon}{\delta\pi}+\frac{\epsilon r\lambda}{\delta\pi}\frac{m}{(m-\rho p)^2}\Big)f'\Big(s_0-\frac{c\epsilon p}{\pi\delta}-\frac{r\lambda\epsilon p}{\pi\delta(m-\rho p)}\Big)\\ &+\frac{r\lambda\rho}{\pi(m-\rho p)^2}\Big(\eta_2 f\Big(s_0-\frac{c\epsilon p}{\pi\delta}-\frac{r\lambda\epsilon p}{\pi\delta(m-\rho p)}\Big)-\epsilon\Big)\\ &\le -\eta_1\Big(\frac{c\epsilon}{\delta\pi}+\frac{\epsilon r\lambda}{\delta\pi}\frac{m}{(m-\rho p)^2}\Big)f'(s)\\ &-\eta_2\Big(\frac{c}{\pi}+\frac{r\lambda}{\pi(m-\rho p)}\Big)\Big(\frac{c\epsilon}{\delta\pi}+\frac{\epsilon r\lambda}{\delta\pi}\frac{m}{(m-\rho p)^2}\Big)f'(s)+\frac{r\lambda\rho}{\pi(m-\rho p)^2}\Big(\eta_2 f(s_0)-\epsilon\Big)\end{aligned}$$

, and thus, by Assumption 1,

$$g'(p)\le 0\quad\forall\ p\in(0,\frac{m}{\rho}).$$

Therefore, the equation $g(p)=0$ admits a unique solution $p_1\in(0,\frac{m}{\rho})$. Thus, we obtain

$$x_1=\frac{\lambda}{m-\rho p_1},\tag{6}$$

$$y_1=\frac{cp_1+\frac{rp_1\lambda}{m-\rho p_1}}{\pi}=\frac{cp_1m-\rho cp_1^2+rp_1\lambda}{\pi(m-\rho p_1)},\tag{7}$$

$$s_1=s_0-\frac{\epsilon}{\delta}\frac{cp_1m-\rho cp_1^2+rp_1\lambda}{\pi(m-\rho p_1)}\le s_0\tag{8}$$

.

Thus, an infected steady-state $E_1=(s_1,y_1,p_1,x_1)$ exists if $\mathcal{R}_0>1$.

Let's show that $E_1\in\overset{\circ}{\Omega}$. From the steady-state conditions of E_1, we have $\Gamma=\delta s_1+\eta_1p_1f(s_1)+\eta_2y_1f(s_1)\to\delta s_1+\epsilon y_1=\Gamma\to 0<s_1<\frac{\Gamma}{\delta}\le M_1$ and $0<y_1<\frac{\Gamma}{\epsilon}\le M_1$.

Using Equations (4) and (5), we obtain

$$cp_1=\pi y_1+\frac{r}{\rho}\lambda-\frac{mr}{\rho}x_1\to cp_1+\frac{mr}{\rho}x_1=\pi y_1+\frac{r}{\rho}\lambda<\pi M_1+\frac{r}{\rho}\lambda$$

, which means that $p_1<\frac{\pi M_1+\frac{r}{\rho}\lambda}{c}\le M_2$ and $x_1<\frac{\rho}{r}\frac{\pi M_1+\frac{r}{\rho}\lambda}{m}\le\frac{\rho M_2}{r}=M_3$.

It follows that $E_1\in\overset{\circ}{\Omega}$. □

2.3. Local Stability

In epidemiology, the basic reproduction number $\mathcal{R}_0$ of an infection is the average number of secondary cases caused by an individual with a communicable disease in a fully susceptible population.

More precisely, $\mathcal{R}_0$ is the average number of people a contagious person can infect. This rate is calculated from a population that is fully susceptible to infection and which has not yet been vaccinated or immunized against an infectious agent.

Theorem 1. *If $\mathcal{R}_0 < 1$, then the disease-free steady-state E_0 is locally asymptotically stable, and if $\mathcal{R}_0 > 1$, it is unstable.*

Proof. The Jacobian matrix at point (s, y, p, x) is given by:

$$J = \begin{pmatrix} -\delta - \eta_1 p f'(s) - \eta_2 y f'(s) & -\eta_2 f(s) & -\eta_1 f(s) & 0 \\ \eta_1 p f'(s) + \eta_2 y f'(s) & \eta_2 f(s) - \epsilon & \eta_1 f(s) & 0 \\ 0 & \pi & -(c + rx) & -rp \\ 0 & 0 & \rho x & \rho p - m \end{pmatrix}.$$

Its value at E_0 is given by:

$$J_0 = \begin{pmatrix} -\delta & -\eta_2 f(s_0) & -\eta_1 f(s_0) & 0 \\ 0 & \eta_2 f(s_0) - \epsilon & \eta_1 f(s_0) & 0 \\ 0 & \pi & -(c + rx_0) & 0 \\ 0 & 0 & \rho x_0 & -m \end{pmatrix}.$$

J_0 admits four eigenvalues; $\lambda_1 = -\delta < 0$ and $\lambda_2 = -m < 0$. λ_3 and λ_4 are eigenvalues of the sub-matrix

$$S_{j_0} := \begin{pmatrix} \eta_2 f(s_0) - \epsilon & \eta_1 f(s_0) \\ \pi & -(c + rx_0) \end{pmatrix}.$$

The trace of S_{j_0} is given by

$$\begin{aligned} \mathrm{Tr}(S_{j_0}) &= \eta_2 f(s_0) - \epsilon - (c + rx_0) \\ &= -(c + rx_0) - \epsilon\Big(1 - \frac{\eta_2 f(s_0)}{\epsilon}\Big) \\ &\leq -(c + rx_0) - \epsilon\Big(1 - \frac{\eta_2 f(s_0)}{\epsilon} - \frac{\pi\eta_1 f(s_0)}{\epsilon(c + rx_0)}\Big) \\ &\leq -(c + rx_0) - \epsilon\Big(1 - \mathcal{R}_0\Big) \end{aligned}$$

and the determinant of S_{j_0} is given by

$$\begin{aligned} \mathrm{Det}(S_{j_0}) &= -(c + rx_0)\Big(\eta_2 f(s_0) - \epsilon\Big) - \pi\eta_1 f(s_0) \\ &= -\epsilon(c + rx_0)\Big(\frac{\eta_2 f(s_0)}{\epsilon} - 1 + \frac{\pi\eta_1 f(s_0)}{\epsilon(c + rx_0)}\Big) \\ &= -\epsilon(c + rx_0)\Big(\mathcal{R}_0 - 1\Big) \\ &= \epsilon(c + rx_0)\Big(1 - \mathcal{R}_0\Big). \end{aligned}$$

Then, the steady-state E_0 is locally asymptotically stable if $\mathcal{R}_0 < 1$, and it is unstable if $\mathcal{R}_0 > 1$. □

Theorem 2. *If $\mathcal{R}_0 > 1$, then the infected steady-state E_1 is locally asymptotically stable.*

Proof. The Jacobian matrix at a point $E_1 = (s_1, y_1, p_1, x_1)$ is given by:

$$J_1 = \begin{pmatrix} -\delta - \eta_1 p_1 f'(s_1) - \eta_2 y_1 f'(s_1) & -\eta_2 f(s_1) & -\eta_1 f(s_1) & 0 \\ \eta_1 p_1 f'(s_1) + \eta_2 y_1 f'(s_1) & \eta_2 f(s_1) - \epsilon & \eta_1 f(s_1) & 0 \\ 0 & \pi & -(c + rx_1) & -rp_1 \\ 0 & 0 & \rho x_1 & \rho p_1 - m \end{pmatrix}.$$

The characteristic polynomial is then given by:

$$P(X) = \begin{vmatrix} -X-\delta-\eta_1 p_1 f'(s_1)-\eta_2 y_1 f'(s_1) & -\eta_2 f(s_1) & -\eta_1 f(s_1) & 0 \\ \eta_1 p_1 f'(s_1)+\eta_2 y_1 f'(s_1) & -X+\eta_2 f(s_1)-\epsilon & \eta_1 f(s_1) & 0 \\ 0 & \pi & -X-(c+rx_1) & -rp_1 \\ 0 & 0 & \rho x_1 & -X+\rho p_1 - m \end{vmatrix}$$

$$= \begin{vmatrix} -(X+\delta) & -(X+\epsilon) & 0 & 0 \\ \eta_1 p_1 f'(s_1)+\eta_2 y_1 f'(s_1) & -X+\eta_2 f(s_1)-\epsilon & \eta_1 f(s_1) & 0 \\ 0 & \pi & -X-(c+rx_1) & -rp_1 \\ 0 & 0 & \rho x_1 & -X+\rho p_1 - m \end{vmatrix}$$

$$= -(X+\delta)\begin{vmatrix} -X+\eta_2 f(s_1)-\epsilon & \eta_1 f(s_1) & 0 \\ \pi & -X-(c+rx_1) & -rp_1 \\ 0 & \rho x_1 & -X+\rho p_1 - m \end{vmatrix}$$

$$+(X+\epsilon)\begin{vmatrix} \eta_1 p_1 f'(s_1)+\eta_2 y_1 f'(s_1) & \eta_1 f(s_1) & 0 \\ 0 & -X-(c+rx_1) & -rp_1 \\ 0 & \rho x_1 & -X+\rho p_1 - m \end{vmatrix}$$

$$= (X+\delta)\Big[(X+\epsilon-\eta_2 f(s_1))\Big((X+c+rx_1)(X+m-\rho p_1)+r\rho p_1 x_1\Big)$$

$$-\pi\eta_1 f(s_1)(X+m-\rho p_1)\Big] + (\eta_1 p_1 f'(s_1)+\eta_2 y_1 f'(s_1))(X+\epsilon)$$

$$\Big((X+c+rx_1)(X+m-\rho p_1)+r\rho p_1 x_1\Big).$$

The characteristic polynomial $P(X) = 0$ if, and only if

$$\Big[(X+\delta)(X+\epsilon-\eta_2 f(s_1))+(\eta_1 p_1 f'(s_1)+\eta_2 y_1 f'(s_1))(X+\epsilon)\Big]$$
$$\Big((X+c+rx_1)(X+m-\rho p_1)+r\rho p_1 x_1\Big) = \pi\eta_1 f(s_1)(X+\delta)(X+m-\rho p_1)$$

or also,

$$\Big[(X+\delta)(X+\epsilon-\eta_2 f(s_1))+(\eta_1 p_1 f'(s_1)+\eta_2 y_1 f'(s_1))(X+\epsilon)\Big] =$$
$$\frac{\pi\eta_1 f(s_1)(X+\delta)(X+m-\rho p_1)}{\Big((X+c+rx_1)(X+m-\rho p_1)+r\rho p_1 x_1\Big)}.$$

Suppose that X is an eigenvalue with $Re(X) \geq 0$; then, since $(\epsilon-\eta_2 f(s_1)) = \frac{\eta_1 p_1 f(s_1)}{y_1}$ and $\frac{p_1}{y_1} = \frac{\pi}{(c+rx_1)}$, the left-hand side satisfies

$$\begin{aligned} \Big|(X+\delta)(X+\epsilon-\eta_2 f(s_1))+(\eta_1 p_1 f'(s_1)+\eta_2 y_1 f'(s_1))(X+\epsilon)\Big| &> (\epsilon-\eta_2 f(s_1))|X+\delta| \\ &= \frac{\eta_1 p_1 f(s_1)}{y_1}|X+\delta| \\ &= \frac{\pi\eta_1 f(s_1)}{c+rx_1}|X+\delta| \end{aligned}$$

, and the right-hand side satisfies

$$\begin{aligned}\left|\frac{\pi\eta_1 f(s_1)(X+\delta)(X+m-\rho p_1)}{(X+c+rx_1)(X+m-\rho p_1)+r\rho p_1 x_1}\right| &< \left|\frac{\pi\eta_1 f(s_1)(X+\delta)(X+m-\rho p_1)}{(X+c+rx_1)(X+m-\rho p_1)}\right| \\ &= \pi\eta_1 f(s_1)\left|\frac{(X+\delta)}{(X+c+rx_1)}\right| \\ &\leq \frac{\pi\eta_1 f(s_1)}{c+rx_1}|X+\delta|.\end{aligned}$$

Hence, the contradiction occurs; thus, $Re(X) < 0$ for all eigenvalues X, and therefore, E_1 is locally asymptotically stable. □

3. Global Stability

Consider the function $G(z) = z - 1 - \ln z$ that will be used in this section.

Theorem 3. *If $\mathcal{R}_0 \leq 1$, then the CHIKV-free equilibrium point E_0 is globally asymptotically stable.*

Proof. Assume that $\mathcal{R}_0 \leq 1$ and define the following Lyapunov function $U_0(s, y, p, x)$:

$$U_0(s, y, p, x) = s - s_0 - \int_{s_0}^{s} \frac{f(s_0)}{f(v)}dv + y + \frac{\eta_1 f(s_0)}{c+rx_0}\left(p + \frac{rx_0}{\rho}G\left(\frac{x}{x_0}\right)\right).$$

Clearly, $U_0(s, y, p, x) > 0$ for all $s, y, p, x > 0$ and $U_0(s_0, 0, 0, x_0) = 0$. The derivative of U_0 with respect to time along the system (1) is given by:

$$\begin{aligned}\dot{U}_0 = &\left(1-\frac{f(s_0)}{f(s)}\right)(\Gamma - \delta s - \eta_1 p f(s) - \eta_2 y f(s)) + \eta_1 p f(s) + \eta_2 y f(s) - \epsilon y \\ &+\frac{\eta_1 f(s_0)}{c+rx_0}\left(\pi y - cp - rxp + \frac{r}{\rho}(1-\frac{x_0}{x})(\lambda + \rho x p - mx)\right) \\ = &\left(1-\frac{f(s_0)}{f(s)}\right)(\Gamma - \delta s) + \eta_1 p f(s_0) + \eta_2 y f(s_0) - \epsilon y \\ &+\frac{\eta_1 f(s_0)}{c+rx_0}\left(\pi y + \frac{r}{\rho}(1-\frac{x_0}{x})(\lambda - mx) - cp - rxp + r(1-\frac{x_0}{x})xp\right)\end{aligned}$$

$$\begin{aligned}\leq &\ \delta\left(1-\frac{f(s_0)}{f(s)}\right)(s_0 - s) + \eta_1 p f(s_0) + \eta_2 y f(s_0) - \epsilon y \\ &+\frac{\eta_1 f(s_0)}{c+rx_0}\left(\pi y + \frac{r}{\rho}(1-\frac{x_0}{x})(\lambda - mx) - p(c+rx_0)\right) \\ \leq &\ \delta\left(1-\frac{f(s_0)}{f(s)}\right)(s_0 - s) + \eta_2 y f(s_0) - \epsilon y + \frac{\eta_1 f(s_0)}{c+rx_0}\left(\pi y + \frac{r}{\rho}(1-\frac{x_0}{x})(\lambda - mx)\right) \\ \leq &\ -\delta\frac{(f(s)-f(s_0))}{f(s)}(s - s_0) + \epsilon\left(\frac{\eta_2 f(s_0)}{\epsilon} + \frac{\pi\eta_1 f(s_0)}{\epsilon(c+rx_0)} - 1\right)y \\ &-\frac{rm\eta_1 f(s_0)}{\rho(c+rx_0)}\frac{(x-x_0)^2}{x} \\ \leq &\ -\delta\frac{(f(s)-f(s_0))}{f(s)}(s - s_0) - \frac{rm\eta_1 f(s_0)}{\rho(c+rx_0)}\frac{(x-x_0)^2}{x} + \epsilon(\mathcal{R}_0 - 1)y.\end{aligned}$$

If $\mathcal{R}_0 \leq 1$, then $\dot{U}_0 \leq 0$ for all $s, y, p, x > 0$. Let $W_0 = \{(s, y, p, x) : \dot{U}_0 = 0\}$. It can be easily shown that $W_0 = \{E_0\}$. Applying LaSalle's invariance principle [30] (see [20,21,31,32] for other applications), we deduce that E_0 is GAS when $\mathcal{R}_0 \leq 1$. □

Theorem 4. *For system (1), if $\mathcal{R}_0 > 1$, then E_1 is **GAS** in $\overset{\circ}{\Omega}$.*

Proof. Let a function $U_1(s, y, p, x)$ be defined as:

$$U_1(s,y,p,x) = s - s_1 - \int_{s_1}^{s} \frac{f(s_1)}{f(v)}dv + y_1 G\left(\frac{y}{y_1}\right) + \frac{\eta_1 p_1 f(s_1)}{\pi y_1} p_1 G\left(\frac{p}{p_1}\right) + \frac{r p_1 \eta_1 f(s_1)}{\rho \pi y_1} x_1 G\left(\frac{x}{x_1}\right).$$

Clearly, $U_1(s, y, p, x) > 0$ for all nonnegative variables $s, y, p, x > 0$ and $U_1(s_1, y_1, p_1, x_1) = 0$. Calculating $\dot{U}_1$ along the solutions of the model (1), we obtain

$$\begin{aligned}
\dot{U}_1 = \; & \left(1 - \frac{f(s_1)}{f(s)}\right)\left(\Gamma - \delta s - \eta_1 p f(s) - \eta_2 y f(s)\right) + \left(1 - \frac{y_1}{y}\right)\left(\eta_1 p f(s) + \eta_2 y f(s) - \epsilon y\right) \\
& + \frac{\eta_1 p_1 f(s_1)}{\pi y_1}\left(1 - \frac{p_1}{p}\right)\left(\pi y - cp - rxp\right) + \frac{r\eta_1 p_1 f(s_1)}{\rho \pi y_1}\left(1 - \frac{x_1}{x}\right)\left(\lambda + \rho x p - mx\right) \\
= \; & \left(1 - \frac{f(s_1)}{f(s)}\right)\left(\Gamma - \delta s\right) - \eta_1 p f(s) - \eta_2 y f(s) + \eta_1 p f(s_1) + \eta_2 y f(s_1) + \eta_1 p f(s) \\
& + \eta_2 y f(s) - \epsilon y - \eta_1 p f(s)\frac{y_1}{y} - \eta_2 y_1 f(s) + \epsilon y_1 + \eta_1 p_1 f(s_1)\frac{y}{y_1} - \eta_1 p_1 f(s_1)\frac{p_1 y}{p y_1} \\
& - \eta_1 p_1 f(s_1)\frac{cp}{\pi y_1} + \eta_1 p_1 f(s_1)\frac{cp_1}{\pi y_1} - \eta_1 p_1 f(s_1)\frac{rxp}{\pi y_1} + \eta_1 p_1 f(s_1)\frac{rxp_1}{\pi y_1} \\
& + \eta_1 p_1 f(s_1)\frac{rxp}{\pi y_1} - \eta_1 p_1 f(s_1)\frac{rx_1 p}{\pi y_1} + \frac{r\eta_1 p_1 f(s_1)}{\rho \pi y_1}\left(1 - \frac{x_1}{x}\right)\left(\lambda - mx\right) \\
= \; & \left(1 - \frac{f(s_1)}{f(s)}\right)\left(\Gamma - \delta s\right) + \eta_1 p f(s_1) + \eta_2 y f(s_1) - \epsilon y - \eta_1 p f(s)\frac{y_1}{y} - \eta_2 y_1 f(s) + \epsilon y_1 \\
& + \eta_1 p_1 f(s_1)\frac{y}{y_1} - \eta_1 p_1 f(s_1)\frac{p_1 y}{p y_1} - \eta_1 p_1 f(s_1)\frac{cp}{\pi y_1} + \eta_1 p_1 f(s_1)\frac{cp_1}{\pi y_1} \\
& + \eta_1 p_1 f(s_1)\frac{rxp_1}{\pi y_1} - \eta_1 p_1 f(s_1)\frac{rx_1 p}{\pi y_1} + \frac{r\eta_1 p_1 f(s_1)}{\rho \pi y_1}\left(1 - \frac{x_1}{x}\right)\left(\lambda - mx\right)
\end{aligned}$$

Applying the steady-state conditions for E_1: $\Gamma = \delta s_1 + \eta_1 p_1 f(s_1) + \eta_2 y_1 f(s_1)$, $\varepsilon y_1 = \eta_1 p_1 f(s_1) + \eta_2 y_1 f(s_1), cp_1 + rx_1 p_1 = \pi y_1, \lambda + \rho x_1 p_1 = m x_1$, we get

$$\begin{aligned}
\dot{U}_1 \; & = -\delta\frac{(s - s_1)(f(s) - f(s_1))}{f(s)} + \left(1 - \frac{f(s_1)}{f(s)}\right)\left(\eta_1 p_1 f(s_1) + \eta_2 y_1 f(s_1)\right) + \eta_1 p f(s_1) \\
& + \eta_2 y f(s_1) - \eta_1 p_1 f(s_1)\frac{y}{y_1} - \eta_2 y f(s_1) - \eta_1 p f(s)\frac{y_1}{y} - \eta_2 y_1 f(s) + \eta_1 p_1 f(s_1) \\
& + \eta_2 y_1 f(s_1) + \eta_1 p_1 f(s_1)\frac{y}{y_1} - \eta_1 p_1 f(s_1)\frac{p_1 y}{p y_1} - \eta_1 p_1 f(s_1)\frac{p(\pi y_1 - r x_1 p_1)}{\pi p_1 y_1} \\
& + \eta_1 p_1 f(s_1)\frac{(\pi y_1 - r x_1 p_1)}{\pi y_1} + \eta_1 p_1 f(s_1)\frac{rxp_1}{\pi y_1} - \eta_1 p_1 f(s_1)\frac{rx_1 p}{\pi y_1} \\
& + \frac{r\eta_1 p_1 f(s_1)}{\rho \pi y_1}\left(1 - \frac{x_1}{x}\right)\left(mx_1 - \rho x_1 p_1 - mx\right) \\
& = -\delta\frac{(s - s_1)(f(s) - f(s_1))}{f(s)} + \left(1 - \frac{f(s_1)}{f(s)}\right)\left(\eta_1 p_1 f(s_1) + \eta_2 y_1 f(s_1)\right) + \eta_1 p f(s_1) \\
& - \eta_1 p_1 f(s_1)\frac{y}{y_1} - \eta_1 p f(s)\frac{y_1}{y} - \eta_2 y_1 f(s) + \eta_1 p_1 f(s_1) + \eta_2 y_1 f(s_1) + \eta_1 p_1 f(s_1)\frac{y}{y_1} \\
& - \eta_1 p_1 f(s_1)\frac{p_1 y}{p y_1} - \eta_1 p f(s_1) + \eta_1 p_1 f(s_1)\frac{r p x_1}{\pi y_1} + \eta_1 p_1 f(s_1) - \eta_1 p_1 f(s_1)\frac{r x_1 p_1}{\pi y_1} \\
& + \eta_1 p_1 f(s_1)\frac{rxp_1}{\pi y_1} - \eta_1 p_1 f(s_1)\frac{rx_1 p}{\pi y_1} - m\frac{r\eta_1 p_1 f(s_1)}{\rho \pi y_1}\frac{(x - x_1)^2}{x} - \eta_1 p_1 f(s_1)\frac{r x_1 p_1}{\pi y_1} \\
& + \eta_1 p_1 f(s_1)\frac{r x_1^2 p_1}{\pi x y_1} \\
& = -\delta\frac{(s - s_1)(f(s) - f(s_1))}{f(s)} + \left(1 - \frac{f(s_1)}{f(s)}\right)\left(\eta_1 p_1 f(s_1) + \eta_2 y_1 f(s_1)\right) - \eta_1 p f(s)\frac{y_1}{y} \\
& - \eta_2 y_1 f(s) + \eta_1 p_1 f(s_1) + \eta_2 y_1 f(s_1) - \eta_1 p_1 f(s_1)\frac{p_1 y}{p y_1} + \eta_1 p_1 f(s_1) \\
& - \eta_1 p_1 f(s_1)\frac{r x_1 p_1}{\pi y_1} + \eta_1 p_1 f(s_1)\frac{rxp_1}{\pi y_1} - m\frac{r\eta_1 p_1 f(s_1)}{\rho \pi y_1}\frac{(x - x_1)^2}{x} \\
& - \eta_1 p_1 f(s_1)\frac{r x_1 p_1}{\pi y_1} + \eta_1 p_1 f(s_1)\frac{r x_1^2 p_1}{\pi x y_1}
\end{aligned}$$

$$
\begin{aligned}
&= -\delta\frac{(s-s_1)(f(s)-f(s_1))}{f(s)} + \eta_1 p_1 f(s_1)\Big(3 - \frac{f(s_1)}{f(s)} - \frac{py_1 f(s)}{p_1 y f(s_1)} - \frac{p_1 y}{py_1}\Big)\\
&+\eta_2 y_1 f(s_1)\Big(2 - \frac{f(s_1)}{f(s)} - \frac{f(s)}{f(s_1)}\Big) - \eta_1 p_1 f(s_1)\frac{rx_1 p_1}{\pi y_1}\Big(2 - \frac{x}{x_1} - \frac{x_1}{x}\Big)\\
&-m\frac{r\eta_1 p_1 f(s_1)}{\rho\pi y_1}\frac{(x-x_1)^2}{x}\\
&= -\delta\frac{(s-s_1)(f(s)-f(s_1))}{f(s)} - \frac{\eta_1 f(s_1) p_1}{\pi y_1}\frac{r\lambda}{\rho x_1}\frac{(x-x_1)^2}{x}\\
&+\eta_2 y_1 f(s_1)\Big(2 - \frac{f(s_1)}{f(s)} - \frac{f(s)}{f(s_1)}\Big) + \eta_1 p_1 f(s_1)\Big(3 - \frac{f(s_1)}{f(s)} - \frac{py_1 f(s)}{p_1 y f(s_1)} - \frac{p_1 y}{py_1}\Big).
\end{aligned}
$$

Using the rule

$$\frac{1}{n}\sum_{i=1}^{n} a_i \geq \sqrt[n]{\prod_{i=1}^{n} a_i}, \tag{9}$$

we get $\frac{1}{2}\Big(\frac{f(s_1)}{f(s)} + \frac{f(s)}{f(s_1)}\Big) \geq 1$ and $\frac{1}{3}\Big(\frac{f(s_1)}{f(s)} + \frac{py_1 f(s)}{p_1 y f(s_1)} + \frac{p_1 y}{py_1}\Big) \geq 1$. Therefore, $\dot{U}_1 \leq 0$ for all $s, y, p, x > 0$ and $\dot{U}_1 = 0$ if, and only if $s = s_1, y = y_1, p = p_1$ and $x = x_1$. Therefore, we deduce that E_1 is globally stable by LaSalle's invariance principle [30] (see [20,21,31,32] for other applications). □

4. Optimal Susceptible Recruitment Rate

Consider a time-varying rate of recruitment of uninfected cells, $\Gamma(t)$ as a control function. Assume further that f is globally Lipschitz with an upper bound $\bar{f} = \sup_{s>0} f(s)$ and a Lipschitz constant L. The control set $\mathbf{P_{ad}}$ is

$$\mathbf{P_{ad}} = \{\Gamma(t) : 0 \leq \Gamma_{\min} \leq \Gamma(t) \leq \Gamma_{\max},\ 0 \leq t \leq T,\ \Gamma(t) \text{ is Lebesgue measurable}\}.$$

The aim is to find the optimal values of $\Gamma(t)$, $s(t)$, $y(t)$, $p(t)$, and $x(t)$ that minimize the criterion function:

$$J(\Gamma) = \int_0^T \Big(-\alpha_1 s(t) + \alpha_2 y(t) + \frac{\alpha_3}{2}\Gamma^2(t)\Big)\, dt.$$

For appropriate positive constants α_1, α_2, and α_3, the aim is to minimize the infected cells and maximize the susceptible ones, while minimizing the control cost.

Since the optimal control problem is linear with respect to the control with bounded states, it is easy to prove the existence of the optimal solution using classical standard results [33].

Existence and Uniqueness of the Solution

Define the variable $\varphi = (s, y, p, x)^t$; then, the model (1) takes the simple form

$$\dot{\varphi} = G(\varphi) = A\varphi + F(\varphi) \tag{10}$$

, where $A = \begin{pmatrix} -\delta & 0 & 0 & 0 \\ 0 & -\varepsilon & 0 & 0 \\ 0 & \pi & -c & 0 \\ 0 & 0 & 0 & -m \end{pmatrix}$ and $F(\varphi) = \begin{pmatrix} \Gamma - pf(s) - yf(s) \\ pf(s) + yf(s) \\ -rxp \\ \lambda + \rho xp \end{pmatrix}$.

Proposition 1. *The function G is continuous and uniformly Lipschitz.*

Proof. The function F is continuous and uniformly Lipschitz, since

$$\begin{aligned}
\|F(\varphi_1) - F(\varphi_2)\|_1 &= \Big| - p_1 f(s_1) - y_1 f(s_1) + p_2 f(s_2) + y_2 f(s_2)\Big| \\
&\quad + \Big|p_1 f(s_1) + y_1 f(s_1) - p_2 f(s_2) - y_2 f(s_2)\Big| + r\Big| - x_1 p_1 + x_2 p_2\Big| + \rho\Big|x_1 p_1 - x_2 p_2\Big| \\
&\leq 2\Big|p_1 f(s_1) + y_1 f(s_1) - p_2 f(s_2) - y_2 f(s_2)\Big| + 2\max(r,\rho)\Big|x_1 p_1 - x_2 p_2\Big| \\
&\leq 2\Big|(p_1 + y_1) f(s_1) - (p_2 + y_2) f(s_2)\Big| + 2\max(r,\rho)\Big|x_1(p_1 - p_2) + p_2(x_1 - x_2)\Big| \\
&\leq 2\Big|(p_1 + y_1) f(s_1) - (p_1 + y_1) f(s_2) + (p_1 + y_1) f(s_2) - (p_2 + y_2) f(s_2)\Big| \\
&\quad + 2\max(r,\rho) M_3\Big|p_1 - p_2\Big| + 2\max(r,\rho) M_2\Big|x_1 - x_2\Big| \\
&\leq 2|p_1 + y_1|\,|f(s_1) - f(s_2)| + 2|f(s_2)|\,|(p_1 + y_1) - (p_2 + y_2)| \\
&\quad + 2\max(r,\rho) M_3\Big|p_1 - p_2\Big| + 2\max(r,\rho) M_2\Big|x_1 - x_2\Big| \\
&\leq 2(M_1 + M_2)\, L|s_1 - s_2| + 2\bar{f}\,(|p_1 - p_2| + |y_1 - y_2|) \\
&\quad + 2\max(r,\rho) M_3\Big|p_1 - p_2\Big| + 2\max(r,\rho) M_2\Big|x_1 - x_2\Big| \\
&\leq M\|\varphi_1 - \varphi_2\|_1
\end{aligned}$$

, where $M = 2\max((M_1 + M_2)\, L, \bar{f}, \bar{f} + M_3 \max(r,\rho), M_2 \max(r,\rho))$. Since

$$\|A\varphi_1 - A\varphi_2\|_1 \leq \|A\|_1 \|\varphi_1 - \varphi_2\|_1 \tag{11}$$

, where $\|A\|_1 := \sup_{X \neq 0} \dfrac{\|AX\|_1}{\|X\|_1}$ is the matrix norm of A subordinate to the vector norm $\|\cdot\|_1$. Therefore,

$$\|G(\varphi_1) - G(\varphi_2)\|_1 \leq K\|\varphi_1 - \varphi_2\|_1 \tag{12}$$

, where $K = \max(M, \|A\|)$, and then the function G is uniformly Lipschitz and continuous. □

Since the function G is uniformly Lipschitz and continuous, then the solution of system (10) exists and is unique.

Let us apply the maximum principle of Pontryagin [33–35] to derive the necessary conditions for the considered optimal control and the corresponding states. The Hamiltonian is

$$\begin{aligned}
H &= -\alpha_1 s + \alpha_2 y + \frac{\alpha_3}{2}\Gamma^2 + \lambda_1 \dot{s} + \lambda_2 \dot{y} + \lambda_3 \dot{p} + \lambda_4 \dot{x} \\
&= -\alpha_1 s + \alpha_2 y + \frac{\alpha_3}{2}\Gamma^2 + \lambda_1(\Gamma - \delta s - p f(s) - y f(s)) + \lambda_2(p f(s) + y f(s) - \epsilon y) \\
&\quad + \lambda_3(\pi y - c p - r x p) + \lambda_4(\lambda + \rho x p - m x).
\end{aligned} \tag{13}$$

For a given optimal control, Γ^*, there exist adjoint functions $\lambda_1, \lambda_2, \lambda_3$ and λ_4 associated to the states s, y, p and x such that:

$$\begin{cases}
\dot{\lambda}_1 &= -\dfrac{\partial H}{\partial s} = \alpha_1 + \lambda_1(\delta + \eta_1 p f'(s) + \eta_2 y f'(s)) - \lambda_2(\eta_1 p f'(s) + \eta_2 y f'(s)), \\
\dot{\lambda}_2 &= -\dfrac{\partial H}{\partial y} = -\alpha_2 + \lambda_1 \eta_2 f(s) + \lambda_2(\varepsilon - \eta_2 f(s)) - \lambda_3 \pi, \\
\dot{\lambda}_3 &= -\dfrac{\partial H}{\partial p} = \lambda_1 \eta_1 f(s) - \lambda_2 \eta_1 f(s) + \lambda_3(c + r x) - \lambda_4 \rho x, \\
\dot{\lambda}_4 &= -\dfrac{\partial H}{\partial x} = \lambda_3 r p + \lambda_4(m - \rho p)
\end{cases} \tag{14}$$

where $\lambda_i(T) = 0$, for $i = 1, 2, 3, 4$, are the transversality conditions.

We minimise the Hamiltonian with respect to the control variable at Γ^*. By using the linearity of the Hamiltonian with respect to the control, we check if the optimal control is bang-bang, singular, or a combination. On the interior of the control set, we have

$$\frac{\partial H}{\partial \Gamma} = \alpha_3 \Gamma + \lambda_1. \tag{15}$$

To investigate the singular case, suppose that $\frac{\partial H}{\partial \Gamma} = 0$, then the singular value is given by

$$\Gamma_{\mathcal{R}msingular}(t) = -\frac{\lambda_1}{\alpha_3}$$

if

$$\alpha_3 \neq 0 \quad \text{and} \quad \Gamma_{\min} \leq -\frac{\lambda_1}{\alpha_3} \leq \Gamma_{\max}.$$

By using the bounds for the control $\Gamma(t)$, we get:

$$\begin{aligned} \text{if } \frac{\partial H}{\partial \Gamma} < 0 \text{ at } t, \text{ then } \Gamma^*(t) &= \Gamma_{\max}, \\ \text{if } \frac{\partial H}{\partial \Gamma} > 0 \text{ at } t, \text{ then } \Gamma^*(t) &= \Gamma_{\min}, \\ \text{if } \frac{\partial H}{\partial \Gamma} = 0, \text{ then } \Gamma_{\mathcal{R}msingular}(t) &= -\frac{\lambda_1}{\alpha_3}. \end{aligned}$$

Hence, the control is optimal at t, provided $\alpha_3 \neq 0$ and $\Gamma_{\min} \leq -\frac{\lambda_1}{\alpha_3} \leq \Gamma_{\max}$.

5. Numerical Results and Conclusions

We used saturated incidence rates of the form $\eta_1 f(s)p$ and $\eta_2 f(s)y$ into this model, where f is a nonlinear increasing function. Thus, the incidence rate considered for numerical simulations is nonlinear and of Monod's type, given by $f(s) = \frac{s}{k+s}$, which is globally Lipschitz with Lipschitz constant $\frac{1}{k}$ where k is a constant.

5.1. Numerical Results for the Direct Problem

We consider the parameters $k = 1, \Gamma = 2, \lambda = 0.1, \pi = 1, \delta = 1, c = 1.2, r = 1, \rho = 0.02$ and $m = 0.6$. For $\epsilon = 0.8, \eta_1 = 1.4$ and $\eta_2 = 2$ then $\mathcal{R}_0 = 4.35 > 1$, the solution of (1) converges to E_1 (Figure 1). This validates the global stability of $E_1 = (s_1, y_1, p_1, x_1)$ when $\mathcal{R}_0 > 1$. For $\epsilon = 1.2, \eta_1 = 0.2$ and $\eta_2 = 0.5$ then $\mathcal{R}_0 = 0.53 < 1$, the solution of (1) converges to $E_0 = (s_0, 0, 0, x_0) = (2, 0, 0, 0.167)$ (Figure 2).

5.2. Numerical Simulations for the Control Problem

For the numerical resolution of the optimal control problem, we applied an appropriated scheme based on a modified Gauss-Seidel-like finite-difference scheme (see Appendix A). The parameter values were the same as in Figure 1 (where the equilibrium E_1 is globally asymptotically stable) but with a variable, Γ. Those values were: $\lambda = 0.1, \pi = 1, \delta = 1, c = 1.2, \epsilon = 0.8, r = 1, \rho = 0.02, m = 0.6, \eta_1 = 1.4, \eta_2 = 2$ and $k = 1$. Here, Γ is a variable such that $\Gamma(0) = 0.1$, $\Gamma^{\min} = 0$ and $\Gamma^{\max} = 10$.

In Figures 3–5, the behaviours of Γ (left), $s(t), y(t), p(t)$ and $x(t)$ (right) were plotted for several values of α_1, α_2, and α_3. As expected, the number of uninfected cells increased and converged to 0; however, the number of infected cells decreased. Figures 3–5 (right) can be compared to Figure 3 in [5], giving the CHIKV pathogenesis.

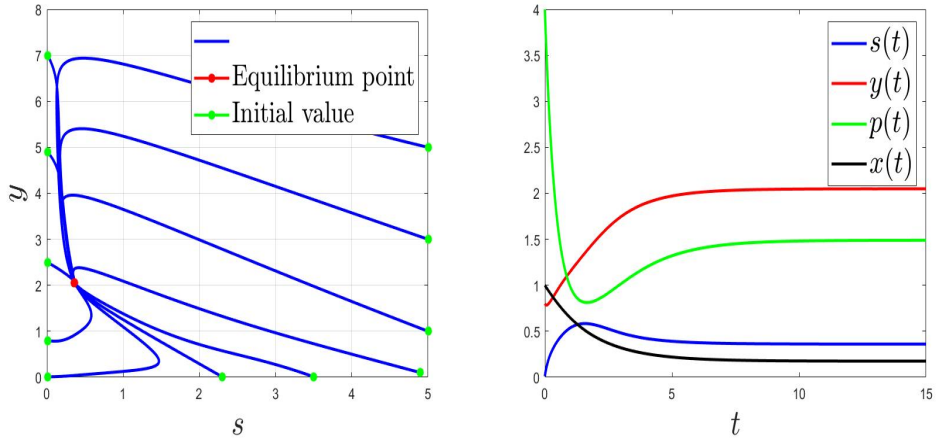

Figure 1. Behaviours for $\epsilon = 0.8, \eta_1 = 1.4$ and $\eta_2 = 2$, then $\mathcal{R}_0 = 4.35 > 1$.

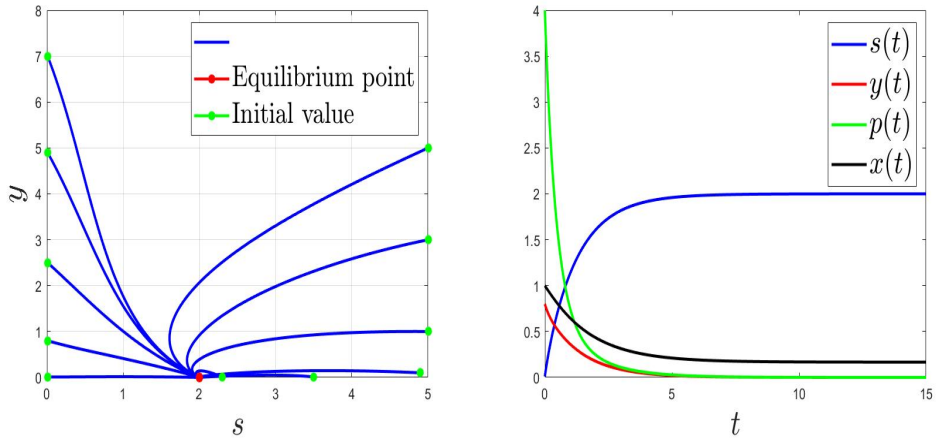

Figure 2. Behaviours for $\epsilon = 1.2, \eta_1 = 0.2$ and $\eta_2 = 0.5$, then $\mathcal{R}_0 = 0.53 < 1$.

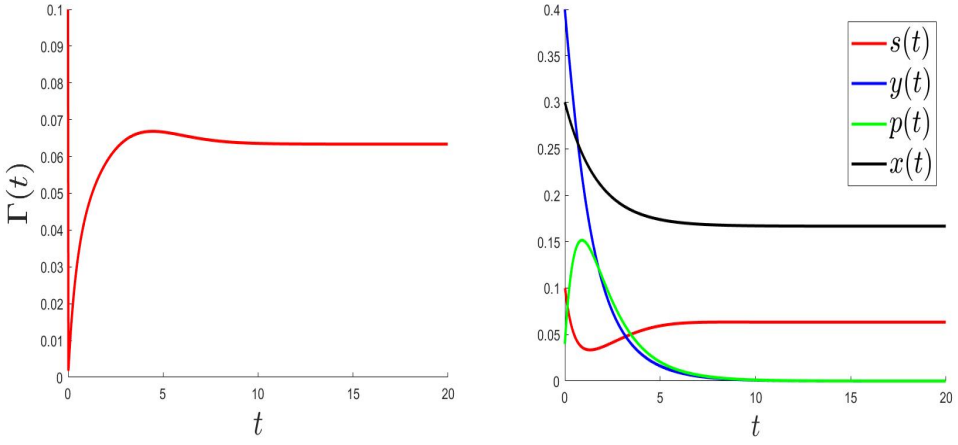

Figure 3. $\alpha_1 = 1, \alpha_2 = 1, \alpha_3 = 10$.

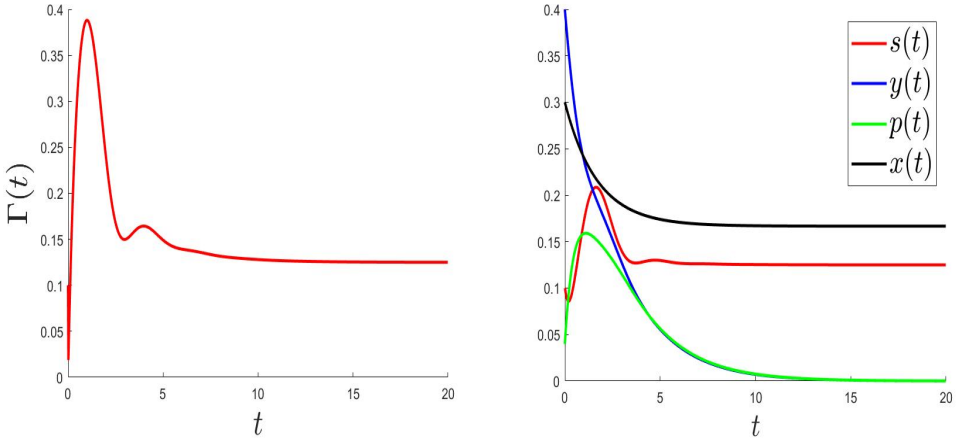

Figure 4. $\alpha_1 = 1, \alpha_2 = 1, \alpha_3 = 1$.

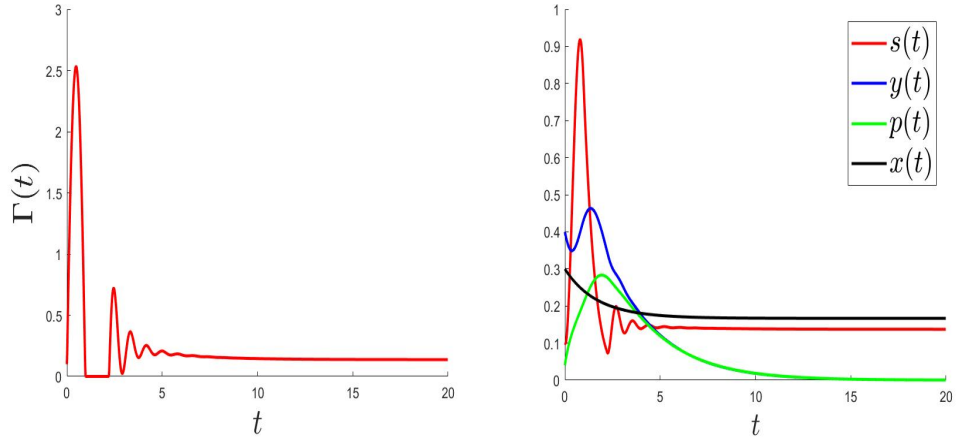

Figure 5. $\alpha_1 = 1, \alpha_2 = 1, \alpha_3 = 0.1$.

6. Conclusions

In the present work, we considered and analyzed a mathematical system of differential equations modelling the Chikungunya virus (CHIKV) dynamics by two ways of infection and general incidence rates. The steady-states, which are the CHIKV-free equilibrium point and CHIKV endemic point, were determined and their local and global stability were studied, based on the basic reproduction number ($\mathcal{R}_0$) obtained by the next-generation matrix. From the analysis, it was found that the disease-free point is locally asymptotically stable if $\mathcal{R}_0 \leq 1$, and the CHIKV endemic point is locally asymptotically stable if $\mathcal{R}_0 > 1$. The global stability of the equilibrium points were carried out using Lyapunov stability, and we confirmed the local stability results. These results are consistent with those obtained when using particular incidence rates as in [18]. We improved and developed the main mathematical techniques used in the previous studies [15–21]. Furthermore, we obtained the same sharp threshold criteria for the local and global stability of both disease-free and endemic steady-states. Later, we applied an optimal recruitment strategy to minimize the number of infected cells. We thus designed a nonlinear optimal control problem. Some numerical simulations were conducted to visualize the analytical results obtained.

There is still a series of questions of great interest. Current scientific research about the dynamics of a virus infection is mainly focused on solving three major issues: the role of time-delay, the space-time spread of a virus outbreak that occurs in a specific region of the territory, and the role of intrinsic fluctuations.

In this context, we can seek to develop a mathematical model which improves the model presented here by considering three types of infected cells, namely, latently infected

cells, short-lived productively infected cells, and long-lived productively infected cells. Such a model can be applied to human immunodeficiency virus (HIV) dynamics.

Author Contributions: Conceptualization, S.A. and S.W.; Methodology, S.A. and S.W.; Writing-original draft, S.A. and S.W.; Writing-review & editing, S.A. and S.W. Both authors have read and agreed to the published version of the manuscript.

Funding: This research received no external funding.

Institutional Review Board Statement: Not applicable.

Informed Consent Statement: Not applicable.

Data Availability Statement: Not applicable.

Acknowledgments: The authors are thankful to the editor and anonymous referees for their valuable comments and suggestions.

Conflicts of Interest: The authors declare no conflict of interest.

Appendix A. Applied Numerical Scheme

Let subdivide the time interval as the following: $[0,T] = \bigcup_{n=0}^{N-1}[t_n, t_{n+1}]$, $t_n = n\ dt$, $dt = T/N$. Let $s^n, y^n, p^n, x^n, \lambda_1^n, \lambda_2^n, \lambda_3^n, \lambda_4^n$ and Γ^n are the approximation of the variables $s(t), y(t), p(t), x(t),\ \lambda_1(t),\ \lambda_2(t), \lambda_3(t), \lambda_4(t)$ and the control $\Gamma(t)$ at time t_n. $s^0, y^0, p^0, x^0, \lambda_1^0, \lambda_2^0, \lambda_3^0, \lambda_4^0$ and Γ^0 are the values of the variables $s(t), y(t), p(t), x(t), \lambda_1(t), \lambda_2(t), \lambda_3(t), \lambda_4(t)$ and the control $\Gamma(t)$ at time $t_0 = 0$. $s^N, y^N, p^N, x^N, \lambda_1^n, \lambda_2^n, \lambda_3^n, \lambda_4^n$ and Γ^n are the values of the variables $s(t), y(t), p(t), x(t), \lambda_1(t), \lambda_2(t), \lambda_3(t), \lambda_4(t)$ and the control $\Gamma(t)$ at time $t_N = T$. The state system was resolved using Gauss-Seidel-like implicit finite-difference method. The adjoint system was resolved using a backward-difference scheme as the following:

$$\begin{cases} \frac{s^{n+1}-s^n}{dt} = \Gamma^n - \delta s^{n+1} - p^n \frac{\eta_1 s^{n+1}}{k+s^n} - y^n \frac{\eta_2 s^{n+1}}{k+s^n}, \\ \frac{y^{n+1}-y^n}{dt} = p^n \frac{\eta_1 s^{n+1}}{k+s^{n+1}} + y^{n+1} \frac{\eta_2 s^{n+1}}{k+s^{n+1}} - \epsilon y^{n+1}, \\ \frac{p^{n+1}-p^n}{dt} = \pi y^{n+1} - c p^{n+1} - r x^n p^{n+1}, \\ \frac{x^{n+1}-x^n}{dt} = \lambda + \rho x^{n+1} p^{n+1} - m x^{n+1}, \\ \frac{\lambda_1^{N-n}-\lambda_1^{N-n-1}}{dt} = \alpha_1 + \lambda_1^{N-n-1}\Big(\delta + \frac{\eta_1 k p^{n+1}}{(k+s^{n+1})^2} + \frac{\eta_2 k y^{n+1}}{(k+s^{n+1})^2}\Big) - \lambda_2^{N-n}\Big(\frac{\eta_1 k p^{n+1}}{(k+s^{n+1})^2} + \frac{\eta_2 k y^{n+1}}{(k+s^{n+1})^2}\Big), \\ \frac{\lambda_2^{N-n}-\lambda_2^{N-n-1}}{dt} = -\alpha_2 + \lambda_1^{N-n-1}\frac{\eta_2 s^{n+1}}{k+s^{n+1}} + \lambda_2^{N-n-1}\Big(\varepsilon - \frac{\eta_2 s^{n+1}}{k+s^{n+1}}\Big) - \lambda_3^{N-n}\pi, \\ \frac{\lambda_3^{N-n}-\lambda_3^{N-n-1}}{dt} = \lambda_1^{N-n-1}\frac{\eta_1 s^{n+1}}{k+s^{n+1}} - \lambda_2^{N-n-1}\frac{\eta_1 s^{n+1}}{k+s^{n+1}} + \lambda_3^{N-n-1}(c + r x^{n+1}) - \lambda_4^{N-n}\rho x^{n+1}, \\ \frac{\lambda_4^{N-n}-\lambda_4^{N-n-1}}{dt} = \lambda_3^{N-n-1} r p^{n+1} + \lambda_4^{N-n-1}(m - \rho p^{n+1}). \end{cases}$$

Hence we applied the algorithm hereafter

Algorithm A1:

1: $s^0 \leftarrow s(0), y^0 \leftarrow y(0), p^0 \leftarrow p(0), x^0 \leftarrow x(0), \lambda_1^N \leftarrow 0, \lambda_2^N \leftarrow 0, \lambda_3^N \leftarrow 0, \lambda_4^N \leftarrow 0,$
$\Gamma^0 \leftarrow \Gamma(0),$

2: **for** $n = 0$ to $N-1$ **do**

$$
\begin{aligned}
s^{n+1} &\leftarrow \frac{s^n + dt\Gamma^n}{1 + dt\left(\delta + \frac{\eta_1 p^n}{k+s^n} + \frac{\eta_2 y^n}{k+s^n}\right)},\\
y^{n+1} &\leftarrow \frac{y^n + dt p^n \frac{\eta_1 s^{n+1}}{k+s^{n+1}}}{1 + dt\left(\epsilon - \frac{\eta_2 s^{n+1}}{k+s^{n+1}}\right)},\\
p^{n+1} &\leftarrow \frac{p^n + dt\pi y^{n+1}}{1 + dt(c + rx^n)},\\
x^{n+1} &\leftarrow \frac{x^n + dt\lambda}{1 + dt(m - \rho p^{n+1})},\\
\lambda_1^{N-n-1} &\leftarrow \frac{\lambda_1^{N-n} + dt\left(-\alpha_1 + \lambda_2^{N-n}\left(\frac{\eta_1 k p^{n+1}}{(k+s^{n+1})^2} + \frac{\eta_2 k y^{n+1}}{(k+s^{n+1})^2}\right)\right)}{1 + dt\left(\delta + \frac{\eta_1 k p^{n+1}}{(k+s^{n+1})^2} + \frac{\eta_2 k y^{n+1}}{(k+s^{n+1})^2}\right)},\\
\lambda_2^{N-n-1} &\leftarrow \frac{\lambda_2^{N-n} + dt\left(\alpha_2 - \lambda_1^{N-n-1}\frac{\eta_2 s^{n+1}}{k+s^{n+1}} + \lambda_3^{N-n}\pi\right)}{1 + dt\left(\epsilon - \frac{\eta_2 s^{n+1}}{k+s^{n+1}}\right)},\\
\lambda_3^{N-n-1} &\leftarrow \frac{\lambda_3^{N-n} + dt\left(-\lambda_1^{N-n-1}\frac{\eta_1 s^{n+1}}{k+s^{n+1}} + \lambda_2^{N-n-1}\frac{\eta_1 s^{n+1}}{k+s^{n+1}} + \lambda_4^{N-n}\rho x^{n+1}\right)}{1 + dt(c + rx^{n+1})},\\
\lambda_4^{N-n-1} &\leftarrow \frac{\lambda_4^{N-n} - dt\lambda_3^{N-n-1} r p^{n+1}}{1 + dt(m - \rho p^{n+1})},\\
\Gamma^{n+1} &\leftarrow \max\left(\min\left(-\frac{\lambda_1^{N-n-1}}{\alpha_3}, \Gamma_{\max}\right), \Gamma_{\min}\right).
\end{aligned}
$$

end

References

1. Kraemer, M.U.; Reiner, R.C.; Brady, O.J.; Messina, J.P.; Gilbert, M.; Pigott, D.M.; Yi, D.; Johnson, K.; Earl, L.; Marczak, L.B.; et al. Past and future spread of the arbovirus vectors Aedes aegypti and Aedes albopictus. *Nat. Microbiol.* **2019**, *4*, 854.
2. Massad, E.; Ma, S.; Burattini, M.N.; Tun, Y.; Coutinho, F.A.B.; Ang, L.W. The risk of chikungunya fever in a dengue-endemic area. *J. Travel Med.* **2008**, *15*, 147–155.
3. Sourisseau, M.; Schilte, C.; Casartelli, N.; Trouillet, C.; Guivel-Benhassine, F.; Rudnicka, D.; Sol-Foulon, N.; Le Roux, K.; Prevost, M.C.; Fsihi, H.; et al. Characterization of reemerging chikungunya virus. *PLoS Pathog.* **2007**, *3*, e89.
4. Ozden, S.; Huerre, M.; Riviere, J.P.; Coffey, L.L.; Afonso, P.V.; Mouly, V.; de Monredon, J.; Roger, J.C.; El Amrani, M.; Yvin, J.L.; et al. Human muscle satellite cells as targets of Chikungunya virus infection. *PLoS ONE* **2007**, *2*, e527.
5. Schwartz, O.; Albert, M. Biology and pathogenesis of chikungunya virus. *Nat. Rev. Microbiol.* **2010**, *8*, 491–500.
6. Alsahafi, S.; Woodcock, S. Mutual inhibition in presence of a virus in continuous culture. *Math. Biosci. Eng.* **2021**, *18*, 3258–3273.
7. Alsahafi, S.; Woodcock, S. Local Analysis for a Mutual Inhibition in Presence of Two Viruses in a Chemostat. *Nonlinear Dyn. Syst. Theory* **2021**, *21*, 337–359.
8. Arora, R.; Kumar, D.; Jhamb, I.; Kaur, Narang, A. Mathematical Modeling of Chikungunya Dynamics: Stability and Simulation. *Cubo* **2020**, *22*, 177–201.
9. Dumont, Y.; Chiroleu, F.; Domerg, C. On a temporal model for the Chikungunya disease: Modeling, theory and numerics. *Math. Biosci.* **2008**, *213*, 80–91.
10. El Hajji, M.; Chorfi, N.; Jleli, M. Mathematical modelling and analysis for a three-tiered microbial food web in a chemostat. *Electron. J. Differ. Equ.* **2017**, *2017*, 1–13.
11. El Hajji, M.; Chorfi, N.; Jleli, M. Mathematical model for a membrane bioreactor process. *Electron. J. Differ. Equ.* **2015**, *2015*, 1–7.

12. El Hajji, M. Boundedness and asymptotic stability of nonlinear Volterra integro-differential equations using Lyapunov functional. *J. King Saud Univ. Sci.* **2019**, *31*,1516–1521.
13. Li, F.; Wang, J. Analysis of an HIV infection model with logistic target cell growth and cell-to-cell transmission. *Chaos Solitons Fractals* **2015**, *81*, 136–145.
14. Long, K.M.; Heise, M.T. Protective and Pathogenic Responses to Chikungunya Virus Infection. *Curr. Trop. Med. Rep.* **2015**, *2*, 13–21.
15. Elaiw, A.M.; Alade, T.O.; Alsulami, S.M. Analysis of latent CHIKV dynamics models with general incidence rate and time delays. *J. Biol. Dyn.* **2018**, *12*, 700–730.
16. Elaiw, A.M.; Alade, T.O.; Alsulami, S.M. Analysis of within-host CHIKV dynamics models with general incidence rate. *Int. J. Biomath.* **2018**, *11*, 1850062.
17. Elaiw, A.M.; Almalki, S.E.; Hobiny, A.D. Global dynamics of Chikungunya virus with two routes of infection. *J. Comput. Anal. Appl.* **2020**, *28*, 481–490.
18. Elaiw, A.M.; Almalki, S.E.; Hobiny, A.D. Global dynamics of humoral immunity Chikungunya virus with two routes of infection and Holling type—II. *J. Math. Computer Sci.* **2019**, *19*, 65–73.
19. Elaiw, A.M.; Almalki, S.E.; Hobiny, A.D. Stability of CHIKV infection models with CHIKV-monocyte and infected-monocyte saturated incidences. *AIP Adv.* **2019**, *9*, 025308.
20. El Hajji, M. Modelling and optimal control for Chikungunya disease. *Theory Biosci.* **2021**, *140*, 27–44.
21. El Hajji, M.; Zaghdani, A.; Sayari, S. Mathematical analysis and optimal control for Chikungunya virus with two routes of infection with nonlinear incidence rate. *Int. J. Biomath.* **2021**, doi:10.1142/S1793524521500881. 2150088.
22. Wang, Y.; Liu, X. Stability and Hopf bifurcation of a within-host chikungunya virus infection model with two delays. *Math. Comput. Simul.* **2017**, *138*, 31–48.
23. Lai, X.; Zou, X. Modeling cell-to-cell spread of HIV-1 with logistic target cell growth. *J. Math. Anal. Appl.* **2015**, *426*, 563–584.
24. Lai, X.; Zou, X. Modelling HIV-1 virus dynamics with both virus-to-cell infection and cell-to-cell transmission. *SIAM J. Appl. Math.* **2014**, *74*, 898–917.
25. Wang, J.; Lang, J.; Zou, X. Analysis of an age structured HIV infection model with virus-to-cell infection and cell-to-cell transmission. *Nonlinear Anal. Real World Appl.* **2017**, *34*, 75–96.
26. Hethcote, H.W. The mathematics of infectious disease. *SIAM Rev.* **2000**, *42*, 599–653.
27. Diekmann, O.; Heesterbeek, J.A.P. On the definition and the computation of the basic reproduction ratio $\mathcal{R}_0$ in models for infectious diseases in heterogeneous populations. *J. Math. Biol.* **1990**, *28*, 365–382.
28. Diekmann, O.; Heesterbeek, J.A.P.; Roberts, M.G. The construction of next-generation matrices for compartmental epidemic models. *J. R. Soc. Interface* **2010**, *7*, 873–885.
29. Van den Driessche, P.; Watmough, J. Reproduction Numbers and Sub-Threshold Endemic Equilibria for Compartmental Models of Disease Transmission. *Math. Biosci.* **2002**,*180*, 29–48.
30. LaSalle, J P. *The Stability of Dynamical Systems*, SIAM: Philadelphia, Pennsylvania, 1976.
31. El Hajji, M.; Sayari, S.; Zaghdani, A. Mathematical analysis of an "SIR" epidemic model in a continuous reactor-deterministic and probabilistic approaches. *J. Korean Math. Soc.* **2021**, *58*, 45–67.
32. El Hajji, M. How can inter-specific interferences explain coexistence or confirm the competitive exclusion principle in a chemostat. *Int. J. Biomath.* **2018**, *11*, 1850111.
33. Fleming, W.H.; Rishel, R.W. *Deterministic and Stochastic Optimal Control*; Springer: New York, NY, USA, 1975.
34. Lenhart, S.; Workman, J.T. *Optimal Control Applied to Biological Models*; Chapman and Hall: London, UK , 2007.
35. Pontryagin, L.S.; Boltyanskii, V.G.; Gamkrelidze, R.V.; Mishchenko, E.F. *The Mathematical Theory of Optimal Processes*; Wiley: New York, NY, USA, 1962.